DOI: 10.13009/EUCASS2019-875

Lift to Drag Ratio, Pitching Moment and Hinge Moment Based Airfoil Optimization

Fazil Selcuk Gomec Berkay Yasin Yildirim* and Ali Oguz Yuksel**
**Aerodynamics Department, Turkish Aerospace*
Ankara 06980, Turkey

Abstract

Airfoil design is extremely important process to reach the optimum flight performance and control parameters. In this paper, a multi objective optimization algorithm will be run for the aspects of flight performance and controllability. Airfoil shape is defined by 5th order Bernstein curves. To create the design space, Latin hypercube sampling method is employed. CFD analyses are performed on the design space and artificial neural networks are trained. Constrained, unconstrained optimization methods, and genetic algorithms are applied to obtain optimum airfoil shapes. Drawbacks and advantages of each optimum output are stated.

1. Introduction

The procedure of aircraft design consists of many complicated system designs which must be provided in a variety of performance requirements. Aerodynamic shape of airfoil is the most fundamental one of these systems. Airfoils are mainly used in cross sections of lifting surfaces of aircraft such as wings, horizontal tails and vertical tails. Different airfoil shapes used in same wing platform and same aircraft configuration cause different flight performance, flight stability, and maneuverability. Hence, designing airfoil becomes important in aircraft design. Airfoil shapes can be optimized to create desired lift, drag, and moment coefficients or characteristics to achieve required flight performance, and stability. In addition, a hinge moment is created on the hinge line where control surfaces are connected to the wing shown in Figure 1. There is a structural limit for this moment due to the material properties. Also, having a linear hinge moment is also important for control surfaces to predict behavior of loads.

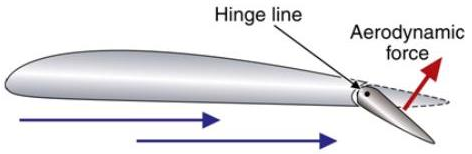

Figure 1. Hinge moment illustration [1]

Drela proposed a sinusoidal based curve system to define the airfoil geometries while Buckley et al. selected B-splines for this purpose [2] [3]. Nemec et al. also adapted B-splines to optimize a multi-element airfoil [4]. Moreover, Gardner and Selig computed airfoil geometries by 7th order Bezier curves [5].

Drela, Vanderplaats and Lyu et al. focused on minimizing the drag coefficient for the multiple objective cases including Mach number, pitch moment, lift coefficient and thickness constraints [2] [6] [7]. Buckley et al. also included maximum lift coefficient at the low subsonic regions as the objective into the optimization system [3].

Zing et al. compared the performances of gradient based and genetic algorithm in aerodynamic shape optimizations. Although the former may converge to local minima and need extra effort for gradient computations, it is advantageous on the latter in the aspect of convergence speed [8]. The method selection can be done with respect to fitness response characteristics. Makinen et al. employed the genetic algorithm for a 2D airfoil optimization problem in the objectives of drag minimization and radar cross section optimization [9]. Kanazaki et al. also adapted the genetic algorithm for a multi-element airfoil design [10]. Kim et al. studied on a gradient-based multi-element airfoil optimization problem for multiple objectives including lift-to-drag, lift and maximum lift issues [11]. In addition, Nemec et al. worked on the drag minimization of a transonic airfoil with a gradient based approach [12].

DOI: 10.13009/EUCASS2019-875

In this study, an initial airfoil geometry is optimized to minimize CD/CL and flap hinge moments and to linearize pitch and flap hinge moments. Optimum values of these parameters provide better flight performance and controllability. An aerodynamic database that represents geometric constraints of the optimization is created. A RANS flow solver, a design of experiment technique and a neural network approach are employed during the database computations. The ready-to-use database enables instant changes in objective functions and optimization algorithms. Instead of creating a database, the airfoil geometry and flow domain would be modified instantly with respect to the gradient values of the objectives. In the case of the modifications in objective functions or optimization methods, many analyses would be repeated or much more analyses would be required for each modification. The ready-to-use aerodynamic database eliminates these disadvantages.

2. Methodology

NACA 63-415 is selected as initial airfoil geometry. The upper and lower section geometries of this airfoil are designed by 5th order Bernstein polynomials. In total, 14 geometric design variables are evaluated in the optimization. These variables sufficiently cover all properties of the airfoil sections. A design space representing these variables is defined by Latin hypercube space filling technique. 2-D flow simulations for this design space is carried out by a RANS flow solver at a subsonic flow regime. The results of CFD simulations are used to train the neural network algorithm. The code NNGA is employed as neural network of this paper. NNGA is an optimized neural network approach that is presented in EUCASS-2017 [13]. 14 different variables are used as input of the airfoil aerodynamic database. Lift, drag, pitch moment and hinge moment differences with respect to the initial airfoil are output of the NNGA. Interior point, SQP and multi-objective genetic algorithm approaches are used for the optimizations. The overview of the optimization methodology of this study is shown in Figure 2.

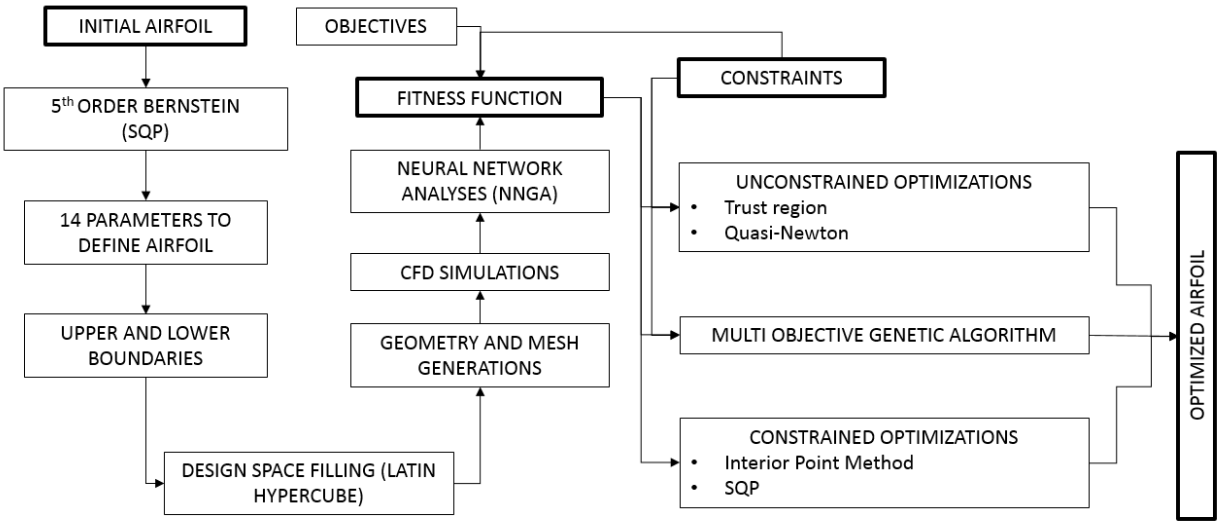

Figure 2. Optimization methodology

2.1 Model

First of all optimization environment is defined. Optimizations are done at 0.2 Mach of air speed. Atmospheric temperature and pressure are selected as 288.15K and 101.325 kPa. 0°, 1°, 3°, 6° and 8° angle of attack values are evaluated at the given Mach number.

The objectives of the optimization process and their related weight and penalty parameters are given in Table *1*. Weight parameters are evaluated in constrained and unconstrained methods while the penalty values are only implemented in the unconstrained one. Weights parameters are used to sum the results of each objectives in the fitness function. Penalty values are employed to limit the geometric parameters in the unconstrained optimization method. Otherwise, it may converge to the out of geometric boundaries which are not trained in neural network analyses. Both factors are not included in the multi objective genetic algorithm.

DOI: 10.13009/EUCASS2019-875

Table 1. Objectives and related weight and penalty factors

NO	OBJECTIVES	WEIGHT	PENALTY VALUE
1	CD is minimized at CL=0.5	0.37	+1
2	Pitch moment coefficient linearity is preserved. Absolute value of (1-R2) linearity is minimized.	0.3	+1
3	Hinge moment coefficient linearity is preserved. Absolute value of (1-R2) linearity is minimized.	0.03	+1
4	Hinge moment value is minimized.	0.3	+1

The constraints defined in the optimization algorithms are given below.

- Airfoil thickness is constrained with $\pm 1\%$ of the initial airfoil thickness due to structural integrity
- The Bernstein curve points of the input airfoil is used as initialization and are limited in X and Y directions. Points are $\pm 30\%$ limited in X-direction and $\pm 10\%$ limited in Y-direction due to manufacturing concerns.
- Trailing edge angle of the airfoil should be between 5°and 15°due to the manufacturing concerns.

2.2 Parametrization of airfoil

For optimization process, first of all, using initial airfoil shape NACA 63415, 5th order Bernstein curve is fitted, and control points are obtained. The upper and lower section geometries of this airfoil are defined as 5th order Bernstein curves. These sections of the airfoil are defined in the equations 1 and 2.

$$\text{UpperSurf.}(x,y)=(1-t)^5P_0+5(t)(1-t)^4P_1+10t^2(1-t)^3P_2+10t^3(1-t)^2P_3+5t^4(1-t)P_4+t^5P_5 \quad [1]$$

$$\text{LowerSurf.}(x,y)=(1-t)^5Q_0+5(t)(1-t)^4Q_1+10t^2(1-t)^3Q_2+10t^3(1-t)^2Q_3+5t^4(1-t)Q_4+t^5Q_5 \quad [2]$$

where t=[0:0.005:0.1 0.11:0.01:1]

Airfoil is defined by two segments that correspond to upper, and lower curves divided from (0, 0) and (chord, 0) coordinates. These points are kept same because they represent leading edge, and trailing edge of the airfoil. There are 4 independent points, and 8 coordinate variables which are x, and y coordinates of the independent points for upper, and lower segment. For upper and lower segments, it corresponds to 16 variables for airfoil shape. However, Q_{11} *and* P_{11} are kept same to have a better leading edge radius which is an important parameter in airfoil design. Hence, final number of variables for airfoil shape is 14 which is used as input variables in optimization process. These variables are shown in Table 2.

Table 2. Variables of 5th order Bernstein curves

	Upper Section			Lower Section	
$\boldsymbol{P_0}$	0	0	Q_0	0	0
$\boldsymbol{P_1}$	0	P_{12}	Q_1	0	Q_{12}
$\boldsymbol{P_2}$	P_{21}	P_{22}	Q_2	Q_{21}	Q_{22}
$\boldsymbol{P_3}$	P_{31}	P_{32}	Q_3	Q_{31}	Q_{32}
$\boldsymbol{P_4}$	P_{41}	P_{42}	Q_4	Q_{41}	Q_{42}
$\boldsymbol{P_5}$	1	-0.0044	Q_5	1	-0.0044

As a result, airfoil shape is represented with Bernstein curves and control points. Figure 3 shows actual initial airfoil shape NACA 63415 with blue points, and its representation with Bernstein curves as red line. As it can be seen from the figure that, airfoil shape is represented correctly with 7 points which have 14 coordinate variables.

DOI: 10.13009/EUCASS2019-875

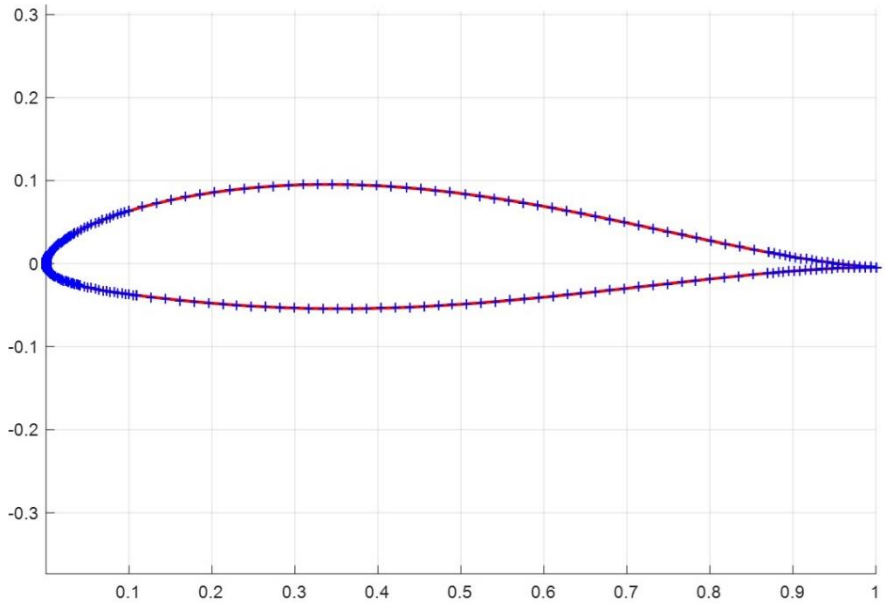

Figure 3. Bernstein curves and airfoil original points.

Since all input parameters for airfoil shape, and flight conditions are known, now the artificial neural networks which correlates outputs to these inputs can be constructed to create an aerodynamic database.

2.3 Design of Experiment

In artificial neural networks, training data is important to accurately create the aerodynamic database. If training data is not appropriate, accuracy decreases dramatically. For this purpose MATLAB® model based calibration functions are evaluated. Latin hypercube sampling function which is called as lhsdesign is used. As a result, 500 different airfoil shapes are created to develop the neural network. This sampling is also done for other input which is angle of attack. Design space of latin hypercube sampling is shown in Figure 4 for first three variables P_{12}, P_{21}, P_{22}.

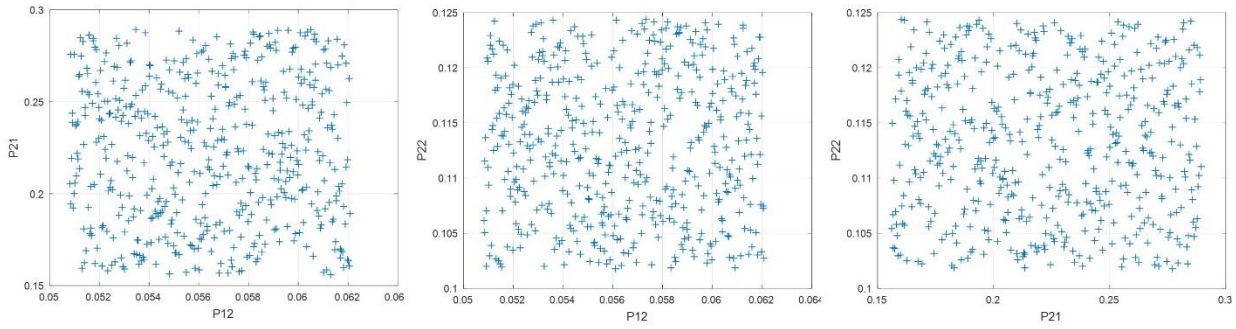

Figure 4. LHS design spaces.

2.4 Mesh Generation

After design space is obtained, to construct the neural networks, outputs are needed. To obtain the results, CFD analyses should be performed which requires mesh generations. Pointwise® mesh generation software is scripted to create meshes with the same parameters for different airfoil shapes which are input variables. Glyph tool of the Pointwise® helps users to create meshing scripts. Computed Bernstein curves are inputs of the program and meshes are created for the corresponding curves. A sample mesh is shown in Figure 5.

DOI: 10.13009/EUCASS2019-875

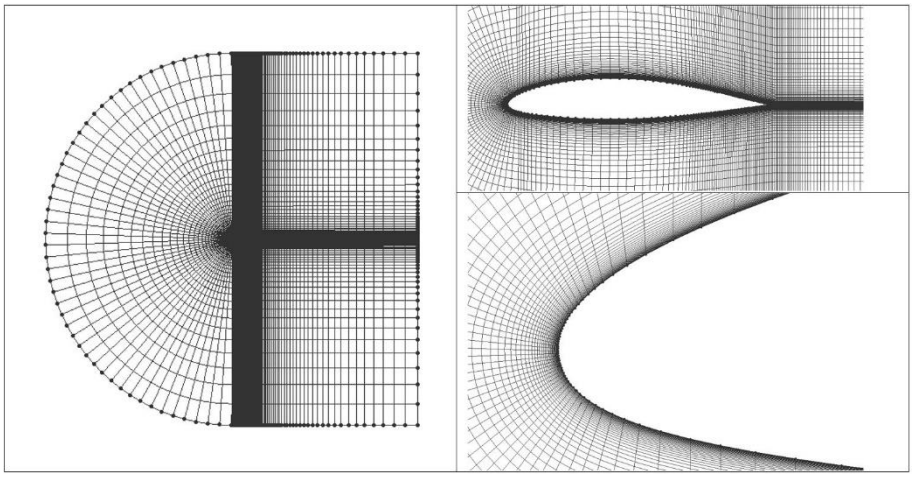

Figure 5. Sample airfoil mesh

2.5 CFD Simulations

CFD simulations are required to obtain outputs which will train neural network algorithm. ANSYS®-Fluent is used to perform 2D CFD simulations. Simulation setup parameters are defined below.

- Turbulence Parameter: Spalart-Allmaras
- Pressure-Velocity Coupling: COUPLED
- Initialization: Standard and FMG Initializations are used.
- Discretization Schemes: 200 iterations using first-order schemes, and 1000 iterations using second-order schemes.

All analyses are performed using ANSYS®-Fluent script which is called as journal file. In this effort, 2500 CFD analyses are performed which take four days to finish all simulations with a 8-core processor. Sample flow fields of the analyses are shown in Figure 6.

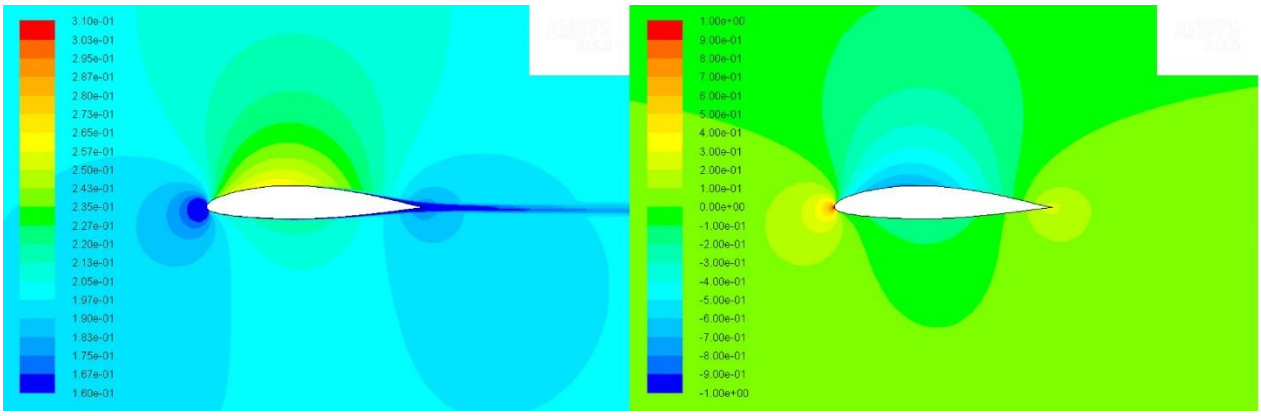

Figure 6. Mach (left) and pressure (right) contours for a sample simulation.

2.6 Artificial Neural Network Construction

Artificial neural networks are created to compute the aerodynamic database of the desired airfoils. The database is required to evaluate fitness functions. The inputs are angles of attack degrees of 0°, 1°, 3°, 6°, 8° and airfoil Bernstein points. Outputs are drag, lift, pitch moment, and hinge moment coefficients. Hinge moment coefficients are taken around 0.7 times chord which is an approximate location for aileron hinge lines. The code NNGA is used as a neural network in this work. NNGA provides an optimized neural network that is presented in EUCASS-2017 [13]. It is a

DOI: 10.13009/EUCASS2019-875

feed forward neural network with Levenberg-Marquard backpropagation algorithm. It has two hidden layers. It optimizes number of neurons in each hidden layer, initial weight, and bias vectors. This NNGA code is only used for creating neural networks that feed the aerodynamic database. The results of NNGA is validated with the aerodynamic database of the initial airfoil. The data of initial airfoil is not used in the network trainings. Results of NNGA validations are shown in Figure 7. As seen from this figure, the outputs aerodynamic database closely match with the test data.

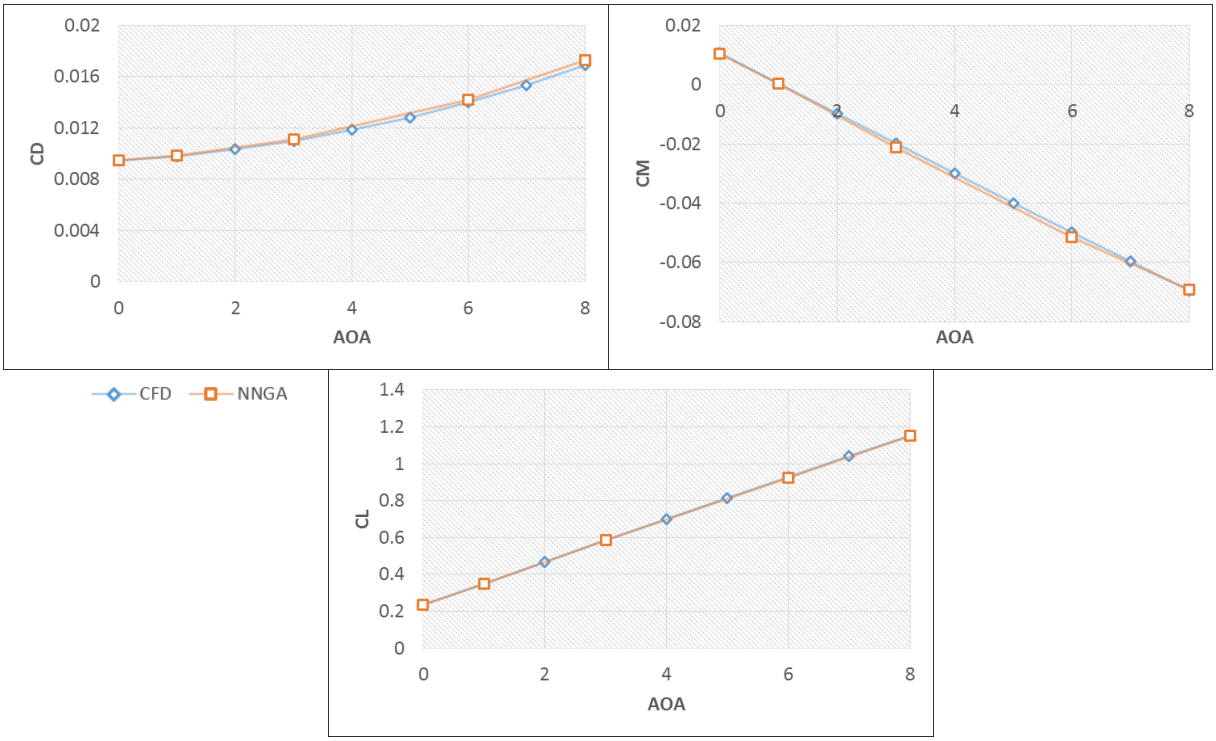

Figure 7. Lift, drag, and pitching moment comparison of actual data, and neural network response surface.

2.7 Optimization

In this study, constrained, unconstrained optimization methods, and a multi objective genetic algorithm are used and compared. MATLAB®'s fminunc, fmincon and gamultiobj functions are used. Interior point, and SQP methods are used as a constrained optimization methods. Quasi-Newton with BFGS Hessian update method is used as an unconstrained optimization method. In these optimization methods, DiffMinChange parameter is selected as 0.0001. Other parameters are kept as default. Default values and parameters are defined as following.

- Function Tolerance: 10e-6
- Optimality Tolerance: 10e-6

Moreover, a multi-objective genetic algorithm is adapted as an optimization approach and following settings are selected for this problem.

- Migration Direction: Forward
- Population Size: 100
- Selection Function: @selectiontournament
- Crossover Fraction: 0.9
- Maximum Generations: 500
- Maximum Stall Generations: 10

DOI: 10.13009/EUCASS2019-875

3. Results and Discussion

Airfoil shape modifications at each iteration of the optimization processes are given in Figure 8.

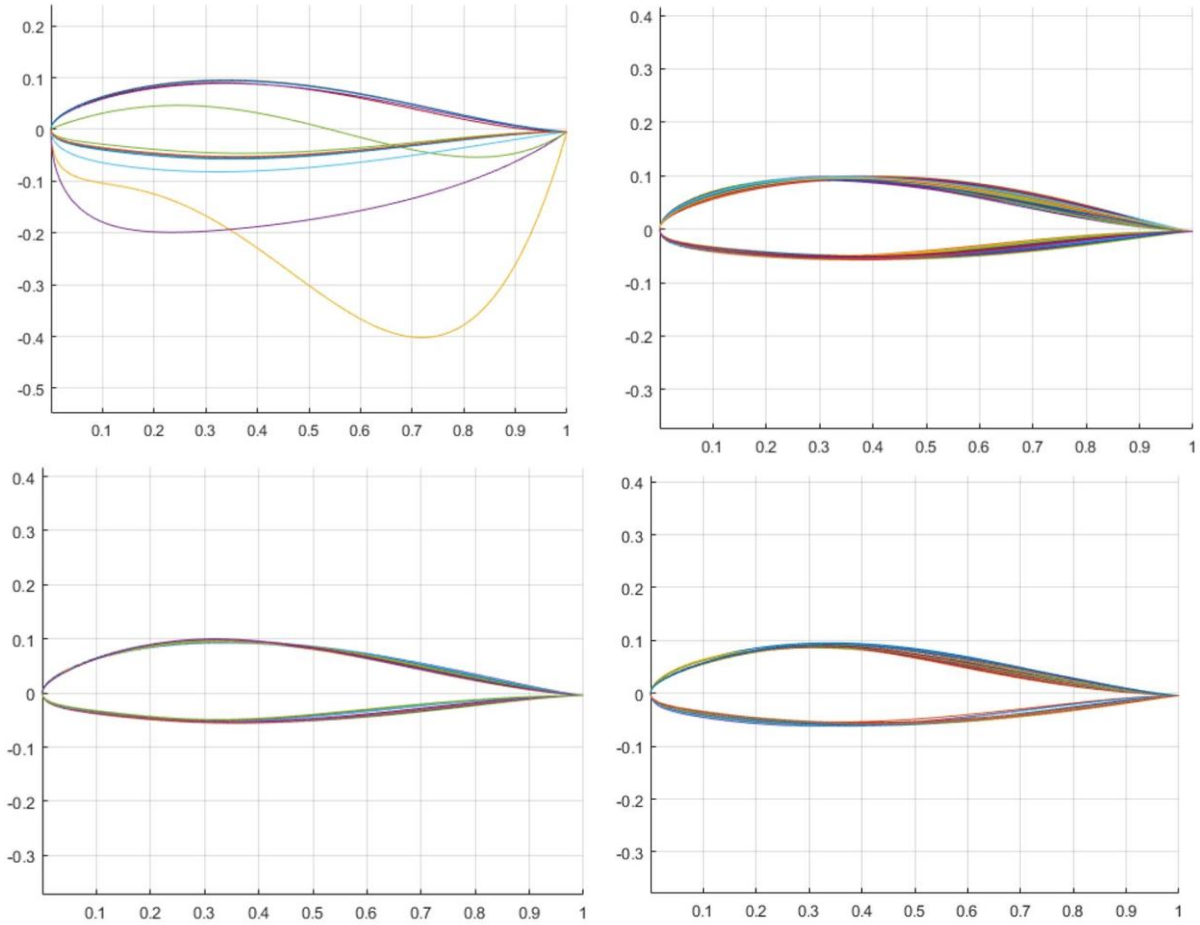

Figure 8. Airfoil shapes at each iteration for Quasi-Newton with BFGS update method (upper-left), Multi Objective Genetic Algorithm (upper-right), Interior Point method (lower-left) and SQP method (lower-right)

As it can be seen from the Figure 8, using unconstrained optimization, some iterations create airfoil shapes that are not feasible. In the constrained optimization methods these points are not feasible and they are not obtained as a result in any iteration. Other methods change the airfoil shape much less in the same regions to achieve optimum.

Convergence of the fitness function for each method is observed, and shown in Figure 9. It can be seen from the figure that, optimization is converged for all methods to a certain minimum value. However, the trend of MOGA is different than other methods because of its algorithm which dynamically changes the populations. In fact, MOGA shows different trends while other methods give reasonable fitness function results, and provide the convergence. It should be noted that the final fitness of MOGA is computed by the fitness formula of other methods. Nevertheless, its fitness is evaluated for each objective independently. As shown in this figure, maximum number of iterations are done for MOGA while the minimum is for SQP. Moreover, the minimum final fitness value is obtained in this method.

DOI: 10.13009/EUCASS2019-875

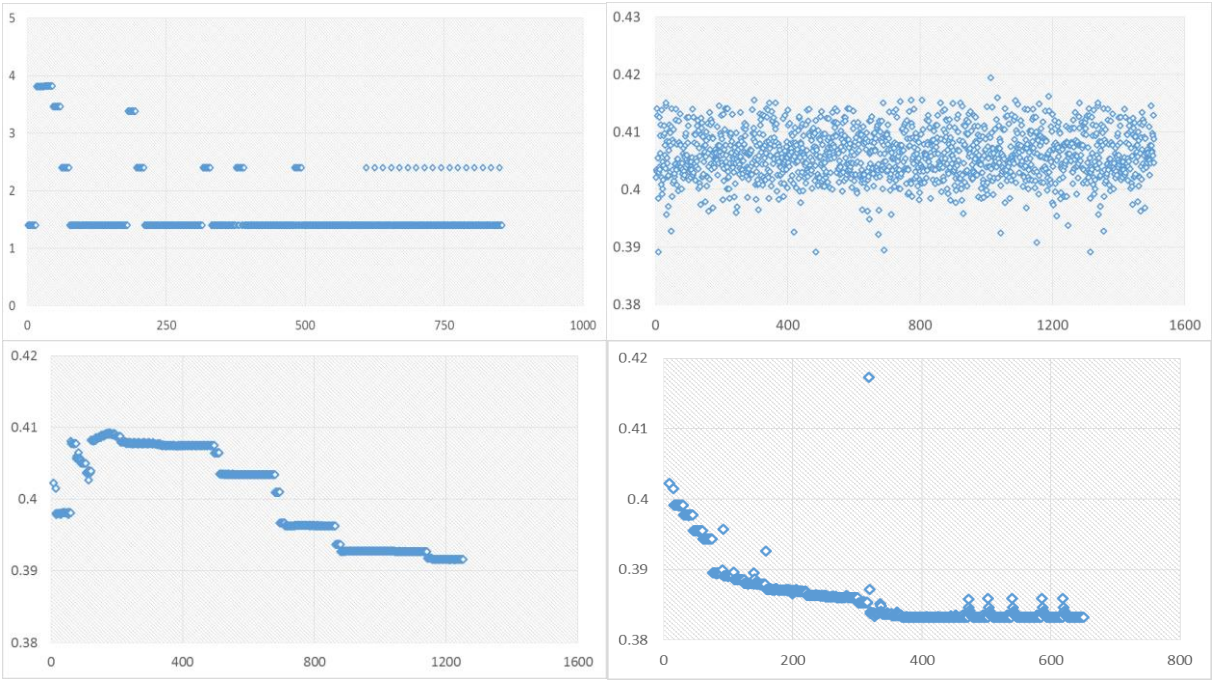

Figure 9. Final fitness function convergence history for Quasi-Newton (upper-left), MOGA (upper-right), IPM (lower-left) and SQP (lower-right).

Optimum airfoil shape Bernstein coordinates are given for each method in Table 3.

Table 3. Optimum airfoil shape Bernstein coordinates

	NACA63415	QN-BFGS	MOGA	IPM	SQP
P12	0.05645	0.05551	0.06104	0.05345	0.05081
P21	0.22276	0.22289	0.24245	0.28692	0.28959
P22	0.11308	0.11162	0.11248	0.12217	0.10179
P31	0.43709	0.43701	0.49266	0.31031	0.30603
P32	0.15700	0.15560	0.16919	0.16334	0.16834
P41	0.73525	0.73494	0.78564	0.70258	0.71460
P42	0.01442	0.01327	0.01362	0.01577	0.01586
P12	-0.05843	-0.05636	-0.05320	-0.05286	-0.05627
P21	0.25000	0.25019	0.23169	0.25686	0.22640
P22	-0.00916	-0.00734	-0.00379	-0.00376	-0.01507
P31	0.27488	0.27492	0.32830	0.26413	0.25882
P32	-0.13095	-0.12933	-0.12417	-0.11902	-0.12315
P41	0.71774	0.71771	0.56864	0.50405	0.91421
P42	-0.00399	-0.00331	-0.00073	-0.00819	-0.00937

DOI: 10.13009/EUCASS2019-875

Result of final airfoil shape, compared with initial airfoil shape is given in Figure 10 for each method.

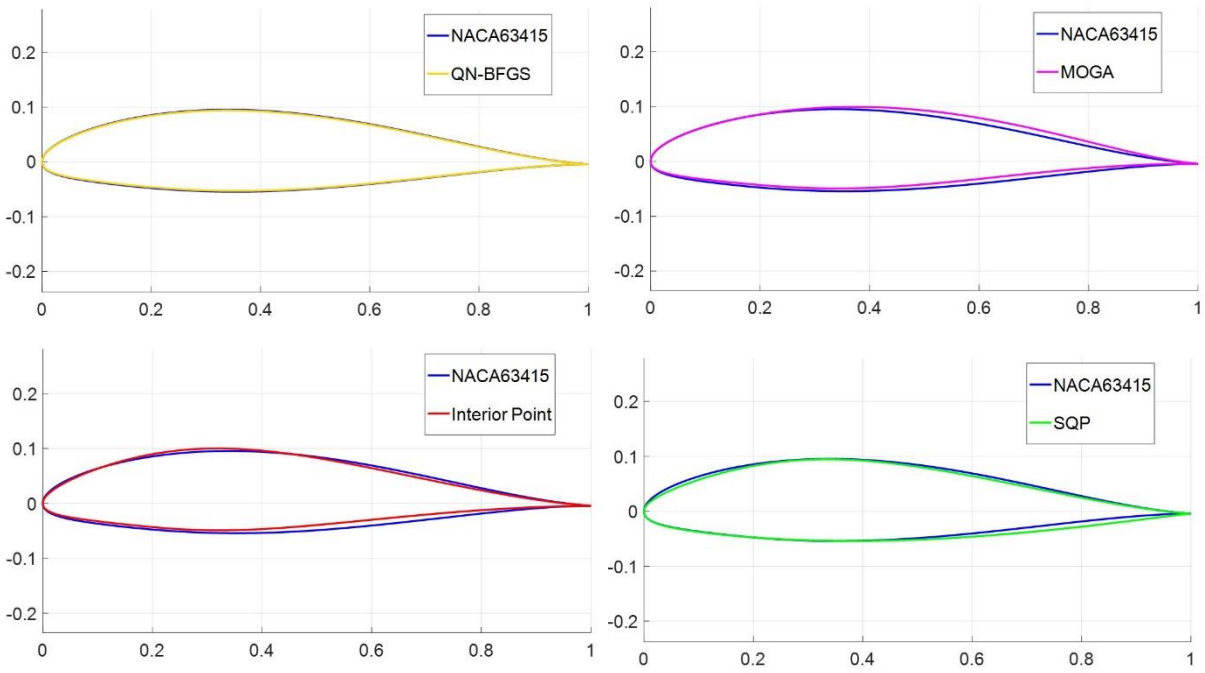

Figure 10. Optimum airfoil shape comparisons for Quasi-Newton with BFGS update method (upper-left), Multi Objective Genetic Algorithm (upper-right), Interior Point method (lower-left) and SQP method (lower-right)

Aerodynamic results of optimum airfoil shapes are given in Figure 11 to check optimum airfoil gives better results or not. As it can be seen from the figure that, optimum airfoil shapes give better performance compared to initial airfoil which proves that optimization is successful.

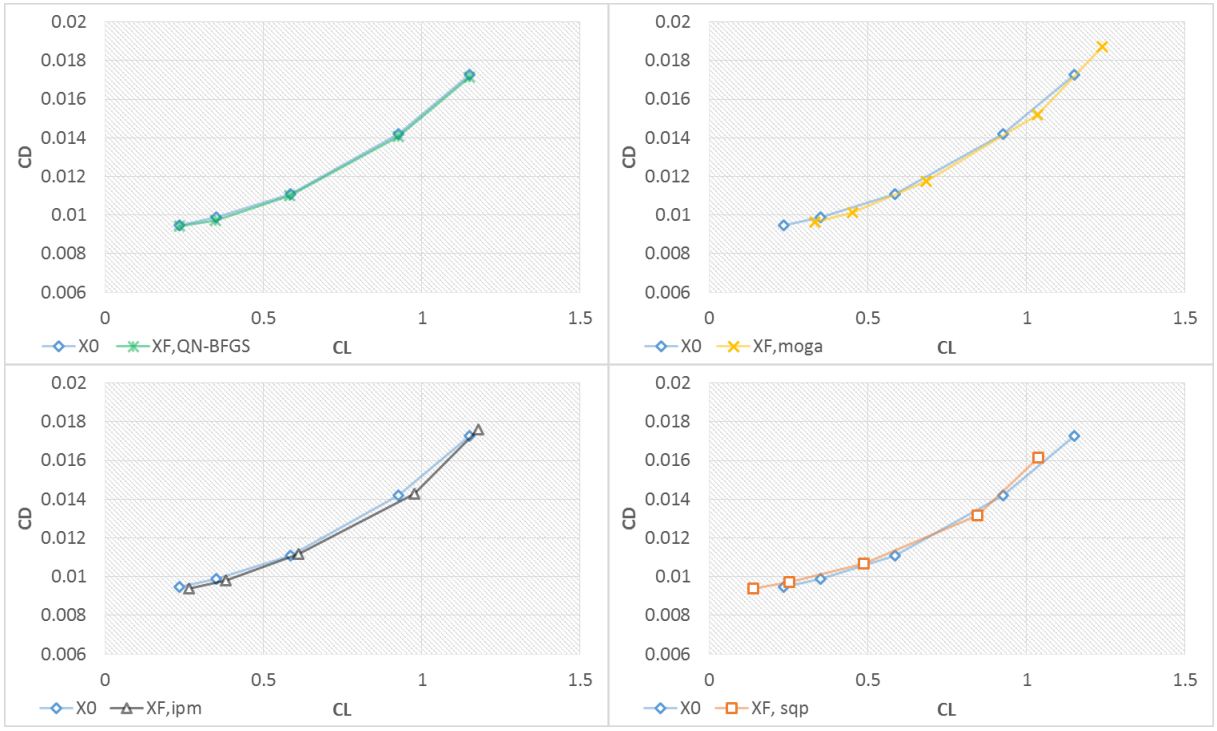

Figure 11. Drag variation with respect to lift of Quasi-Newton (upper-left), MOGA (upper-right), IPM (lower-left) and SQP (lower-right)

DOI: 10.13009/EUCASS2019-875

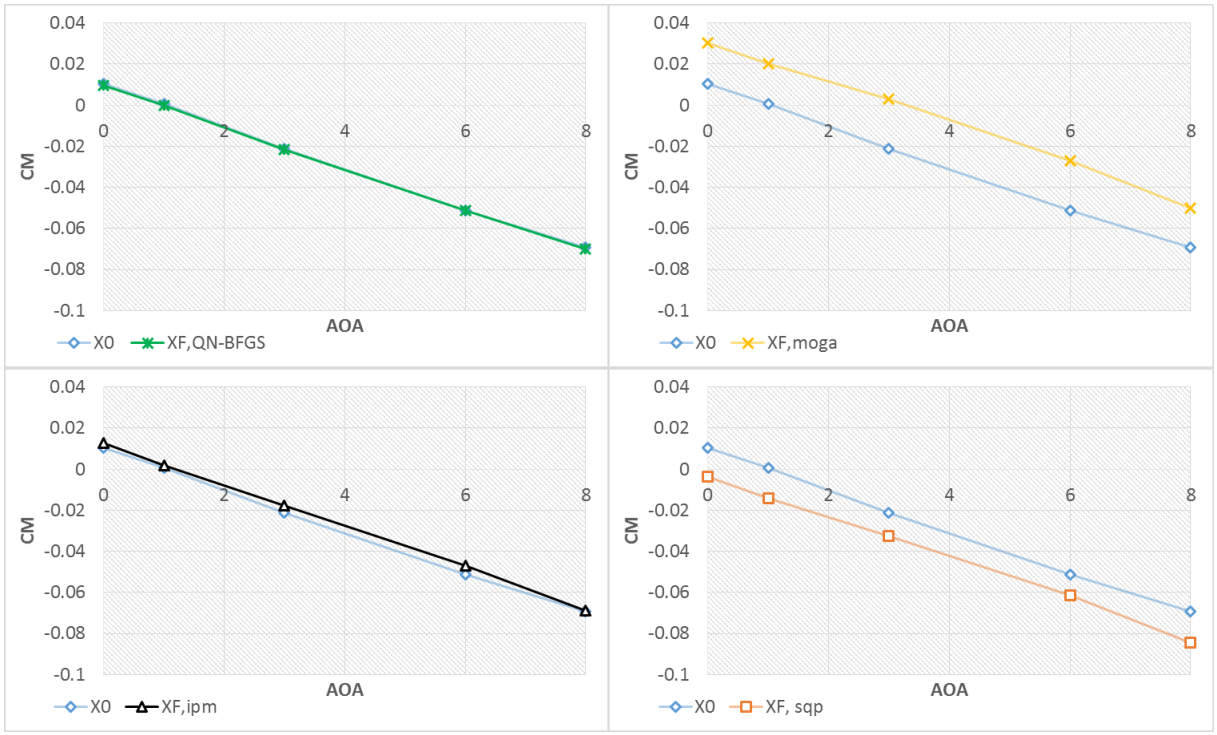

Figure 14: Pitch moment variation with respect to angle of attack of Quasi-Newton (upper-left), MOGA (upper-right), IPM (lower-left) and SQP (lower-right)

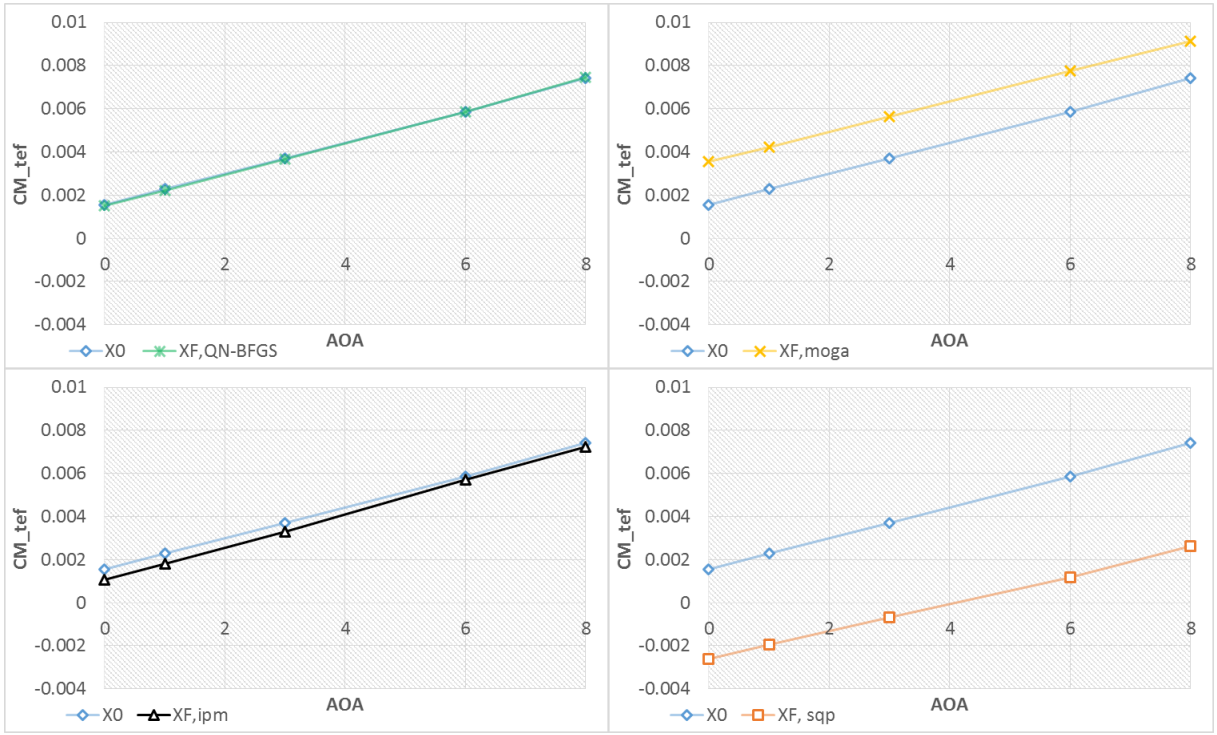

Figure 15: Flap hinge moment variation with respect to angle of attack of Quasi-Newton (upper-left), MOGA (upper-right), IPM (lower-left) and SQP (lower-right)

DOI: 10.13009/EUCASS2019-875

4. Conclusion

For the selected initial airfoil geometry, 5th order Bernstein parameters are defined and a design space that includes the initial airfoil is created. CFD runs are performed on this design space. An artificial neural network is trained with these CFD analyses. This network is used as a database generator. Optimization runs are done by different algorithms including multi-objective, single-objective with multi-weighted, constrained and unconstrained methods.

The optimization results are highly dependent to the fitness weights for single output fitness functions. Different weights may lead eliminating one of the objectives. The weights of each objective is found by some iterative computations. The neural networks provide possibility for testing new weights almost in a second.

It is easily shown that Quasi-Newton method converges nearly to the geometry of the initial geometry. The unconstrained method could not find better points than the original airfoil geometry. Penalty factors lead this unsuccessful result. Drag to lift ratio characteristics of NACA 64315 is improved by interior point method and multi-objective genetic algorithm while it is slightly decreased by SQP. The best performances for pitch moment and flap hinge moment linearity are obtained by interior point method. The maximum value of flap hinge moment is decreased significantly with SQP method. The reason of smallest final fitness value is reasoned by this result. Although interior point method's final fitness is slightly higher than the one of SQP, it showed the best outputs since it provides improvement in all objectives.

References

[1] "Aviation Supplies and Academics," The Pilot's Manual Ground School, 2009. [Online]. Available: https://slideplayer.com/slide/10804459. [Accessed 02 2019].

[2] M. Drela , "Pros and Cons of Airfoil Optimization," in *Frontiers of Computational Fluid Dynamics*, World Scientific, 1998.

[3] H. Buckley, B. Zhou and D. Zingg, "Airfoil Optimization Using Practical Aerodynamic Design Requirements," in *27th AIAA Applied Aerodynamics Conference*, San Antonio, Texas, 2009.

[4] M. Nemec, D. Zingg and T. Pulliam, "Multipoint and Multi-Objective Aerodynamic Shape Optimization," *AIAA Journal*, vol. 42, no. 06, 2004.

[5] B. Gardner and M. Selig, "Airfoil Design Using a Genetic Algorithm and an Inverse Method," in *41st Aerospace Sciences Meeting and Exhibit*, Reno, Nevada, 2003.

[6] G. Vanderplaats, "Approximation Concepts for Numerical Airfoil Optimization," NASA Technical Paper-1370, California, 1979.

[7] Z. Lyu, G. Kenway and J. Martins, "Aerodynamic Shape Optimization Investigations of the Common Research Model Wing Benchmark," *AIAA Journal*, vol. 53, no. 04, 2015.

[8] D. Zingg, M. Nemec and T. Pulliam, "A comparative evaluation of genetic and gradient-based algorithms applied to aerodynamic optimization," *REMN*, vol. 17, pp. 103-126, 2008.

[9] R. Makinen and J. Toivanen, "Multidisciplinary Shape Optimization in Aerodynamics and Electromagnetics using Genetic Algorithms," *Int. J. Numer. Meth. Fluids*, vol. 30, pp. 149-159, 1999.

[10] M. Kanazaki, K. Tanaka, S. Jeong and K. Yamamoto, "Multi-objective Aerodynamic Optimization of Elements' Setting for High-lift Airfoil Using Kriging Model," in *44th AIAA Aerospace Sciences Meeting and Exhibit*, Reno,Nevada, 2006.

[11] S. Kim, J. Alonso and A. Jameson, "Multi-Element High-Lift Configuration Design Optimization Using Viscous Continuous Adjoint Method," *Journal of Aircraft*, vol. 41, no. 5, 2004.

[12] M. Nemec and M. Aftosmis , "Aerodynamic Shape Optimization Using a Cartesian Adjoint Method and CAD Geometry," in *24th AIAA Applied Aerodynamics Conference*, San Fransico, CA, 2006.

[13] F. Gomec and M. Canibek, "Aerodynamic Database Improvement of Aircraft based on Neural Networks and Genetic Algorithms," in *7TH European conference for Aeronautics and Space Sciences (EUCASS)*, Milano, 2017.